# Identification and Localization of Slow, Natural, Cooperative Unfolding in the Hematopoietic Cell Kinase SH3 Domain by Amide Hydrogen Exchange and Mass Spectrometry†

John R. Engen,‡ Thomas E. Smithgall,§ William H. Gmeiner,§ and David L. Smith*,‡,§

*Department of Chemistry, University of Nebraska−Lincoln, Lincoln, Nebraska 68588-0304, and Eppley Institute for Research in Cancer and Allied Diseases, University of Nebraska Medical Center, Omaha, Nebraska 68198-6805*

*Received July 7, 1997; Revised Manuscript Received September 15, 1997*⊗

ABSTRACT: Protein unfolding on a fast time scale (milliseconds−minutes) has been widely reported, but slower unfolding events (10 min−hours) have received less attention. Amide hydrogen exchange (HX) and mass spectrometry (MS) were used to investigate the unfolding dynamics of the hematopoietic cell kinase (Hck) SH3 domain. Analysis of mass spectra after deuterium exchange into intact Hck SH3 indicates a cooperative unfolding event involving 24−61% of the domain and occurring with a half-life of approximately 20 min under physiological conditions. To identify the unfolding region, SH3 was incubated in $D_2O$ and proteolytically fragmented into peptides that were analyzed by mass spectrometry. Correlation of HX rates and isotope patterns reveals cooperative unfolding in several regions, including the C-terminal half of the RT-loop and a $\beta$-sheet flanking the binding site. Binding of a prolyl-rich segment from the HIV Nef protein slows unfolding by a factor of 3. Further analysis yields a $K_D$ of 25 $\mu$M for the Nef peptide. These results demonstrate that an inherent flexibility in the SH3 domain may assist interconversion of the closed, intramolecularly ligated state and the open, active state of Src family kinases. Furthermore, this type of previously undetectable, slow unfolding process may provide the basis for new mechanisms in which kinetics of local unfolding combines with thermodynamics to regulate enzymatic activity. The combination of hydrogen exchange and mass spectrometry appears to be the only general method capable of examining these slow unfolding processes.

Protein dynamics is essential for proper function of a large number of proteins (representative examples include refs 1−6). Some proteins, such as transcriptional activators (*6*), undergo global changes from a highly disordered, nonfunctional form to a correctly folded and functional form. Others, such as a 131-residue fragment from staphylococcal nuclease (*7*), exist in a partially folded state and make a final transition to the native state in the presence of substrate. Countless other proteins undergo localized conformational changes while performing their functions. The rates at which these structural changes occur is likely to influence the activity of the protein. In larger, complex signaling proteins, such as tyrosine kinases, small domains participate in structural changes required for activation of the larger molecule. Two of these domains, the Src homology 2 (SH2[1]) and 3 (SH3) domains (for a review see ref 8), have been of particular interest because of their roles in controlling kinase activity. SH2 domains bind sequences containing phosphotyrosine and, with approximately 100 residues, are the larger of the two. SH3 domains have approximately 60 residues, which form five $\beta$-strands to create a hydrophobic binding surface for proline-rich sequences containing the PxxP motif. The binding surface is flanked by two connecting loops, the RT-loop and the n-Src-loop.

Recent reports of the structures of the Hck and c-Src tyrosine kinases (*9*, *10*) illustrate the importance of interdomain interactions in regulating protein function. Interactions between the SH3 domain and a previously unrecognized type II polyproline helix located in the linker region between the SH2 and kinase domains are now believed to partially control the catalytic activity of Src family tyrosine kinases. Kinase activity can be altered when other ligands compete with the SH2−kinase linker for SH3. Of particular interest is HIV Nef, which binds tightly to the Hck SH3 domain *in vitro* (*11*). Nef−SH3 interaction is sufficient to stimulate Hck kinase activity *in vitro* (*12*) and release Hck tyrosine kinase and transforming activities in rodent fibroblasts (*13*). To understand how interdomain interactions such as these contribute to protein function, we must identify thermodynamic and kinetic factors affecting ligand interchange. The present study focuses on the slow unfolding kinetics of the Hck SH3 domain.

While there appear to be no reports of dynamics studies on intact Hck or any other tyrosine kinase, a small number of reports have been made on the dynamics of SH3 domains. Bruton's tyrosine kinase SH3, α-spectrin SH3, and *Caenorhabditis elegans* Sem-5 SH3 were induced to unfold with

† This work was supported by NIH Grant R01 GM40384 to D.L.S., NIH Grant R01 CA58667 to T.E.S., NIH Grant R01 CA60612 to W.H.G., NIH Grant P30 CA36727, the Nebraska Department of Health, and the Nebraska Center for Mass Spectrometry. J.R.E. was partially supported by a fellowship from the Nebraska Center for Biotechnology.

* Author to whom correspondence should be addressed at Department of Chemistry, University of Nebraska-Lincoln, Lincoln, NE 68588-0304. Tel: (402) 472-2794. Fax: (402) 472-9862. E-mail: dls@unlinfo.unl.edu.

‡ University of Nebraska-Lincoln.

§ Eppley Institute.

⊗ Abstract published in *Advance ACS Abstracts,* November 1, 1997.

[1] Abbreviations: Hck, hematopoietic cell kinase; SH3, Src homology 3; SH2, Src homology 2; HX, hydrogen exchange; MS, mass spectrometry; HIV, human immunodeficiency virus; Nef, negative factor; NefP, HIV Nef peptide (residues 69−80); NMR, nuclear magnetic resonance; ESIMS, electrospray ionization mass spectrometry.

S0006-2960(97)01635-8 CCC: $14.00 

heat, denaturants, or pH to determine their stability (*14*−*16*). Results indicate that the SH3 domain, which is approaching the lower size limit postulated by Privalov for a stable folded unit (*17*), has high thermal stability but normal to low stability at ambient temperatures. In other work, NMR studies have shown that an approximate 1:1 ratio of folded:unfolded protein exists at pH 7 for the N-terminal SH3 domain of the adapter protein Drk. The unfolding rate constant was reported to be 0.89 $s^{-1}$ (*18*, *19*). The N-terminal SH3 domain from Grb2, the mammalian homologue of Sem-5 and Drk, displayed similar behavior at pH 3.5 (*20*). Drk SH3 showed little variation in dynamics across the backbone (*21*), and Drk binding to a target peptide decreased the dynamics and increased the stability of the domain (*22*). Other much faster movements of SH3 have also been characterized by NMR (*23*−*26*), molecular dynamics simulations (*27*), and X-ray crystallography B-factors (*28*−*30*). Although unfolding processes in the 1-s time range, such as for Drk SH3, can be investigated by NMR spectroscopy, they represent the slow end of the NMR time scale. Slower unfolding processes can be detected by loss of activity or various spectroscopic measurements. However, these approaches generally do not lead to identification of specific regions participating in the unfolding process. Localized unfolding of proteins on a slower time scale (minutes−hours) has not been studied, primarily because there has been no effective method to detect slow unfolding processes.

We report here a new approach, based on amide hydrogen exchange and mass spectrometry (HX−MS), for investigating the dynamics of proteins over a wide time range. While amide hydrogen exchange detected by NMR has become invaluable for investigating the dynamics and thermodynamics of localized protein unfolding and refolding (as examples, see refs 31−34), amide hydrogen exchange detected by mass spectrometry has received somewhat less attention. HX−MS has been used to determine exchange rates for intact polypeptides (*35*, *36*) and fragments of intact proteins (*37*−*39*) and to detect structural heterogeneity (*39*−*41*). Slow, natural, cooperative unfolding of the Hck SH3 domain in aqueous solution at pH 7 was examined using this approach. We show how HX/protein fragmentation can be used to localize unfolding to short segments of the backbone and how binding of this SH3 domain to a segment of HIV Nef alters the unfolding rate. These results suggest that localized unfolding of the SH3 domain on the minute time scale may play a role in regulating catalytic activity of Hck and may indicate a mechanism through which HIV Nef stimulates Hck kinase activity *in vivo*. The combination of hydrogen exchange and mass spectrometry offers the possibility for revealing slow unfolding processes and localized dynamics in a wide range of proteins.

## MATERIALS AND METHODS

*Materials.* Recombinant Hck SH3 was prepared by amplifying a cDNA fragment encoding residues 77−143 of human Hck SH3 with PCR and subcloning it into the T7-based bacterial expression vector pET14b. *Escherichia coli* strain BL21 (DE3) pLysS was transformed with this vector and grown at 37 °C in M9 minimal medium. After the optical density (600 nm) reached 0.8, protein expression was induced by addition of 0.4 mM IPTG. At 4 h after induction, cells were collected by centrifugation and lysed by sonication. The cell lysate was clarified by centrifugation and purified by anion-exchange chromatography (High-Q, Bio-Rad). Proteins were eluted with a linear gradient of 0−500 mM NaCl. Fractions containing the SH3 protein were combined and further purified on a Sephacryl S-200 size-exclusion column to a purity of >95% as determined by SDS−PAGE. The average molecular mass was determined by ESIMS to be 8231 Da (calculated value 8231 Da). The 12-mer HIV Nef peptide (PVRPQVPLRPMT) (as in ref 11) was synthesized by the University of Nebraska-Lincoln Protein Core Facility using standard techniques and purified by reversed-phase HPLC. Its molecular mass was verified by ESIMS. Fully deuterated Hck SH3 in which all exchangeable hydrogens were replaced with deuterium was prepared by incubating SH3 in $D_2O$ at pH 6.9 for 5 h at 37 °C followed by incubation for 24 h at room temperature.

*Deuterium Exchange In.* Hydrogen-exchange experiments were similar to those previously reported (*38*, *41*, *42*). For analysis of the SH3 domain alone, a master solution was prepared by equilibrating 100 nmol of Hck SH3 in 10 $\mu$L of 100 mM phosphate buffer (pH 6.9) at 22 °C for 100 min. Deuterium exchange was initiated by diluting the master solution 20-fold with 5 mM phosphate buffer, pH 6.9, $D_2O$. At each time point, ∼3 nmol was removed from the master solution, diluted 8-fold into 100 mM phosphate buffer, pH 2.5, $H_2O$ to quench isotopic exchange, and placed at −70 °C until analysis. One tube of master solution as just described was adequate to prepare samples for analysis at 15 time points. For SH3 domain incubated with HIV Nef peptide (NefP), 10 $\mu$L of 9.5 nmol/$\mu$L NefP in 100 mM phosphate buffer, pH 6.9, $H_2O$ was added to 100 nmol of Hck SH3 and allowed to equilibrate for 100 min. Based on a $K_D$ of 90 $\mu$M (*11*), 79% of SH3 was bound to NefP. Deuterium exchange was performed as described for SH3 alone.

*Analysis of Intact Protein.* Mass spectra of intact SH3 were acquired with a Micromass Platform mass spectrometer coupled to capillary perfusion HPLC; 10 $\mu$L (650−700 pmol) of sample (0 °C) was injected onto a 100-mm × 0.25-mm (i.d.) perfusion column (POROS 10 R2 media, PerSeptive Biosystems) operating at a flow rate of 40 $\mu$L/min. Protein was eluted with a gradient of 15−98% acetonitrile in 3.5 min. The injector and column were cooled to 0 °C to minimize deuterium back-exchange. With each set of samples, an undeuterated ($m_{0\%}$) control and a totally deuterated ($m_{100\%}$) control were also analyzed to adjust for deuterium back-exchange during analysis (*38*). Equation 1 was used to apply this correction, where $D$ is the deuterium content of the protein, $m$, $m_{0\%}$, and $m_{100\%}$ are the average molecular weights of the same protein in the partially deuterated or sample form, the undeuterated form, and the totally deuterated form, respectively, and $N$ is the number of peptide amide hydrogens in the protein:

$$D = \frac{m - m_{0\%}}{m_{100\%} - m_{0\%}} \times N \qquad (1)$$

The HPLC step was performed with protiated solvents, thereby removing deuterium from side chains and amino/carboxy termini that exchange much faster than amide linkages (*43*). Therefore, an increase in mass was a direct measure of deuteration at peptide amide linkages. Duplicate analyses were performed for each time point. Data presented are transformed spectra from the original charge distributions.

The centroids of isotope envelopes in bimodal patterns were determined by fitting the data with two Gaussian functions whose widths were estimated from the width of single binomial isotopic envelope before and after the appearance of the bimodal pattern. The unfolding rate constants were determined from the slope of pseudo-first-order kinetic plots of the decrease in the relative intensity of the lower mass envelope with time.

*Pepsin Digestion and Fragment Analysis.* Deuterium exchange in was performed as described above. Before analysis, 10 $\mu$L (400−450 pmol) of each sample was incubated with 5 $\mu$L of a 1 $\mu$g/$\mu$L pepsin solution for 5 min at 0 °C. The peptides were fractionated in 7 min by a 5−60% acetonitrile−water gradient using reversed-phase perfusion HPLC as for intact protein analysis. The $m_{0\%}$ and $m_{100\%}$ controls were also digested and eq 1 used to adjust for the loss of deuterium from the peptides during analysis. Analyses were performed with a Micromass Autospec high-resolution mass spectrometer equipped with focal plane detector and standard electrospray interface. Data were processed by centroiding an isotopic distribution corresponding to the +1, +2, or +3 charge state of each peptide. Since peptic cleavage sites are difficult to predict accurately, all peptide mass assignments were confirmed by analysis of molecular weight information (*38*, *44*), MS/MS techniques (*45*), and carboxy-terminal sequencing (*46*, *47*). Deuterium levels were plotted versus the exchange in time and fitted with a series of first-order rate expressions according to eq 2, where $D$ is the number of deuterium present, $N$ is the number of peptide amide linkages in a segment, and $k_i$ is the hydrogen deuterium-exchange rate constant for each peptide linkage (*41*). The exchange rate constants, $k_i$, were varied to obtain the best fit between the experimental data and eq 2. The exchange experiment was performed in triplicate and each time point analyzed in duplicate.

$$D = N - \sum_{i=1}^{N} \exp(-k_i t) \tag{2}$$

*Nef Peptide Concentration Study and Determination of $K_D$.* Apparent unfolding rate constants, $k_{app}$, were determined for SH3 incubated with various concentrations of HIV Nef peptide (5−8910 $\mu$M), as described for intact protein analysis. Data were plotted as $1/k_{app}$ vs free peptide concentration and fitted with eq 3, where $k_1$ is the rate constant for unfolding from the unbound form, $k_1'$ is the rate constant for unfolding from the bound form, [P] is the free peptide concentration, and $K_D$ is the equilibrium dissociation constant (*48*).

$$\frac{1}{k_{app}} = \frac{K_D + [P]}{k_1 K_D + k_1'[P]} \tag{3}$$

## RESULTS

The model for localized hydrogen exchange (eq 4) from transiently unfolded proteins has been reviewed elsewhere (*31*−*34*, *39*). Replacement of hydrogen with deuterium may occur from locally unfolded forms ($U_H$) of a protein in equilibrium with folded forms ($F_H$). The rate constants $k_1$, $k_{-1}$, and $k_2$ describe unfolding, refolding, and hydrogen exchange, respectively. Deuterated forms of the unfolded and folded protein are designated by $U_D$ and $F_D$, respectively.

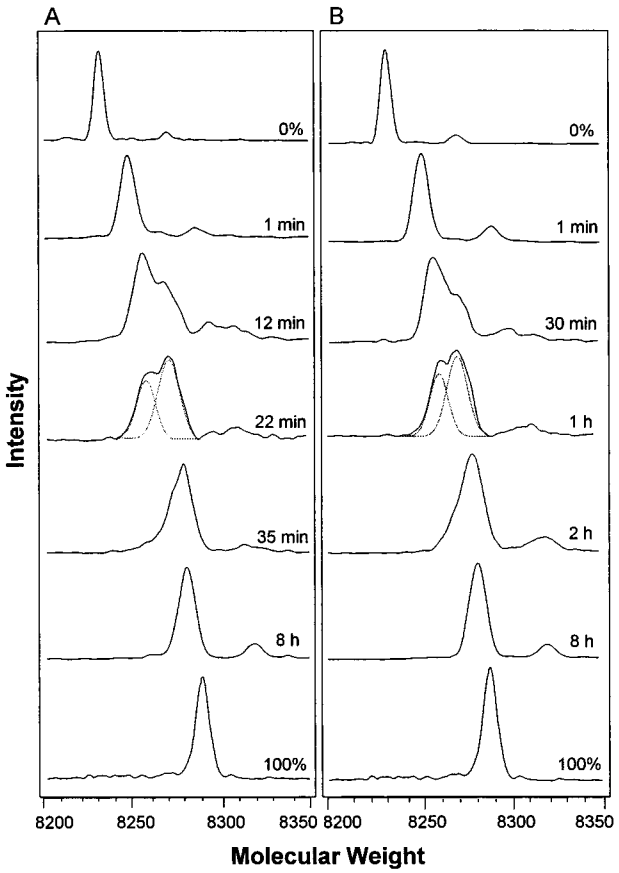


FIGURE 1: Electrospray mass spectra of intact human Hck SH3 domain incubated in $D_2O$ alone (A) and with HIV Nef peptide (B). The incompletely resolved experimental data were fitted with two Gaussian functions, (A) for 22 min and (B) for 1 h. The fraction of molecules remaining folded at any time is given by the area of the low-mass envelope of isotope peaks. The average molecular weight, given by the centroid of each envelope, was used to determine the deuterium level for each incubation time (*38*).

$$F_H \underset{k_{-1}}{\overset{k_1}{\rightleftharpoons}} U_H \xrightarrow[D_2O]{k_2} U_D \underset{k_1}{\overset{k_{-1}}{\rightleftharpoons}} F_D \tag{4}$$

Hydrogen exchange from unfolded states has two kinetic limits: EX1 and EX2. When EX1 kinetics prevails, $k_{-1} \ll k_2$. Isotopic exchange is complete in unfolded regions before they refold. Under EX2 kinetics, $k_{-1} \gg k_2$, the protein must make many short visits to the unfolded state before isotopic exchange is complete. For proteins under physiological conditions, HX usually occurs by EX2 kinetics but may occur via a combination of the two limits, as demonstrated below for Hck SH3. The extent to which HX occurs by EX1 or EX2 kinetics can be clearly distinguished from the distribution of isotope peaks in mass spectra. A random distribution of deuterium among the sample molecules, detected as a single binomial distribution of isotope peaks in mass spectra, indicates HX by EX2 kinetics. Bimodal distributions of isotope peaks are the most direct evidence for EX1 kinetics (*40*). It is noted that exchange directly from the folded form, as discussed by Woodward et al., also results in a single binomial distribution of isotopes (*34*, *49*).

*Unfolding of Intact SH3.* Mass spectra obtained for intact SH3 following incubation in $D_2O$ are presented in Figure 1A. For incubation times less than 7 min, single binomial distributions of isotope peaks were found indicating EX2 kinetics. For incubation times in the 7−30-min range, bimodal isotope patterns were found indicating EX1 kinetics.

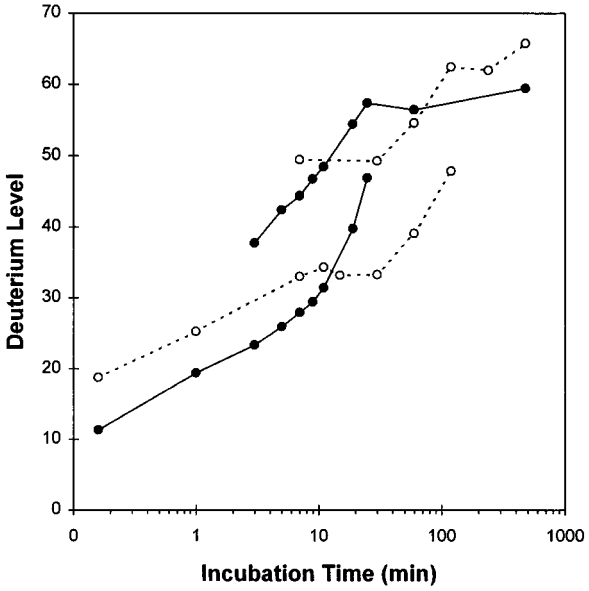


FIGURE 2: Deuterium levels found in intact SH3 incubated in $D_2O$ alone (solid line) or with HIV Nef peptide (dotted line). The amount of deuterium gained was determined from the centroid of the isotopic envelopes in Figure 1 at each exchange in time. The lower and upper lines represent forms of SH3 that have not and have undergone partial cooperative unfolding, respectively.

At longer incubation times, mass spectra again indicated a single binomial distribution of deuterium among the SH3 molecules. Deuterium levels determined from these spectra are presented as a function of incubation time in Figure 2. The deuterium level gradually increased from 11 to 23 as the incubation time increased from 1 to 3 min. Deuterium levels found in the low- and high-mass isotope envelopes of bimodal isotope patterns in the 7−30-min range are also indicated in Figure 2. The lower and upper mass envelopes in the bimodal isotope pattern represent the folded and unfolded forms of SH3, respectively. The term unfolded is used to describe species that have unfolded to allow correlated exchange at some time during the incubation in $D_2O$. The rate constant for the localized unfolding event, determined from the decrease in the area of the low-mass envelope with $D_2O$ incubation time, is 0.04 $min^{-1}$ ($t_{1/2}$ 17 min). These results show that a region within the SH3 domain undergoes cooperative unfolding such that the rate constant for refolding ($k_{-1}$) is much less than the intrinsic rate constant for hydrogen exchange ($k_2$). For our experimental conditions, the average $k_2$ at any peptide amide linkage is 350 $min^{-1}$ (calculated from ref 43).

The minimum number of residues involved with the cooperative unfolding event was determined from the difference between the centroids of the low- and high-mass isotope envelopes (Figure 2). After adjustment for deuterium loss during analysis (*38*), this difference was 17, indicating that at least 17 amide linkages are directly involved in the unfolding process. Seventeen represents the lower bound in the size of the region undergoing cooperative unfolding because amide linkages that were both completely deuterated via EX2 exchange prior to the cooperative unfolding event and participating in cooperative unfolding would not contribute to the mass difference of the two envelopes. For incubation times of 7−30 min, the mass of both envelopes increased due to hydrogen exchange via EX2 kinetics at amide hydrogens outside the cooperative unfolding region.

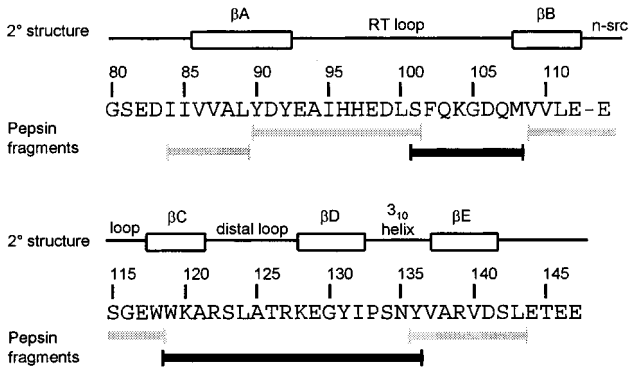


FIGURE 3: Human Hck SH3 numbered according to the chicken c-Src sequence. Secondary structural elements determined by X-ray crystallography (*9*) are shown above the sequence. Fragments produced by peptic digestion are shown below. Black shading indicates peptic fragments of SH3 that are most involved in the cooperative unfolding event.

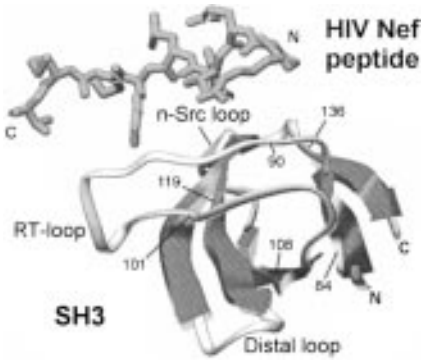


FIGURE 4: Ribbon diagram prepared from the X-ray structure of Fyn SH3 and HIV NefP (*50*). Residues 3−12 of the HIV Nef peptide that was used in this study are shown binding between the RT- and n-Src-loops of Fyn SH3. Fyn SH3 is the most homologous SH3 domain to Hck that has coordinates in the Brookhaven Protein Data Bank (ID 1EFN). Numbering is according to the chicken c-Src sequence and indicates key residues in pepsin digestion.

However, the mass difference between the two envelopes remained constant during the first part of this time interval, indicating that peptide amide hydrogens within the unfolding region did not exchange appreciably via EX2 kinetics on this time scale. As the incubation time approached 30 min, the mass difference between the two envelopes decreased, consistent with some HX beginning to occur within the unfolding region via EX2 kinetics. When the partially unfolded form first appeared, its molecular weight was ∼28 Da less than that of completely exchanged SH3, indicating that at least 28 residues were not involved with the cooperative unfolding event. Since there are 72 amide linkages in the SH3 domain, cooperative unfolding must involve fewer than 44 residues.

*Unfolding Region Identified by Peptic Fragments.* To identify regions involved in the cooperative unfolding, intact SH3 was incubated in $D_2O$ and digested with pepsin, yielding six fragments covering 82% of the Hck SH3 backbone (Figure 3). Hydrogen-exchange rates and isotope patterns for each of the fragments were used to localize the unfolding region to specific short fragments of the SH3 backbone. The position of these segments in the tertiary structure, illustrated in Figure 4, is based on the X-ray crystal structure of Fyn SH3 (*50*), the most homologous SH3 domain for which there are coordinates in the Brookhaven Protein Data Bank. Sicheri et al. reported that the tertiary structure of Fyn SH3

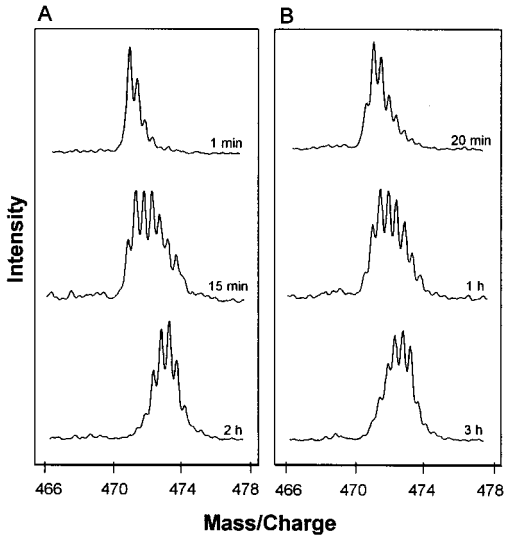


FIGURE 5: Incorporation of deuterium by the 101−108 fragment of Hck SH3. SH3 was incubated alone (A) and with 8.9 mM HIV Nef peptide (B). Mass spectra shown are for the +2 charge state of fragment 101−108.

is virtually identical to Hck SH3, as determined by X-ray crystallography of intact Hck (*9*). To facilitate comparison with previous work on SH3 domains, the Hck SH3 sequence has been numbered according to the chicken c-Src sequence.

Mass spectra of segments of Hck SH3, determined by HPLC ESIMS, appeared either binomial or bimodal, indicating EX2 or EX1 kinetics. Results for the 101−108 fragment are shown in Figure 5. The isotope patterns found in mass spectra of the fragment including residues 101−108 (Figure 5A) appear bimodal, a characteristic feature of EX1 kinetics. It is significant that the appearance of this bimodal isotope pattern occurs within the same time frame as the appearance of the bimodal pattern found for intact SH3 (Figure 1A). The isotope pattern for fragment 119−136 also appears bimodal in the same time frame (data not shown). Isotope patterns for the remaining segments appear binomial, indicating EX2 kinetics (data not shown). These results suggest that regions of the backbone including residues 101−108 and 119−136 are involved with the slow, cooperative unfolding event illustrated by results presented in Figure 1A.

Deuterium levels in each segment, determined by HPLC ESIMS, are presented in Figure 6. If residues within these segments were involved with the cooperative unfolding event, the deuterium level in the segment would increase for incubation times near the unfolding half-life determined for intact SH3 (17 min as indicated by vertical solid lines in Figure 6). Fitting residues 84−89 (Figure 6A) to a series of first-order rate expressions (*41*) shows that all of the peptide amide hydrogens in this segment exchange with half-lives of 135 min, which is significantly greater than 17 min. Hence, this segment cannot be involved with the cooperative unfolding event. Similar data analysis for the other five segments (Figure 6B−F) shows that each segment has at least a few peptide amide hydrogens with exchange half-lives near 17 min. Segments including residues 101−108 (Figure 6C) and 119−136 (Figure 6E) have the largest number of amide hydrogens likely to be involved with cooperative unfolding. Since the cooperative unfolding event includes at least 17 residues, and since the number of amide hydrogens from segments 101−108 and 119−136 that exchange at the appropriate rate accounts for fewer than 14

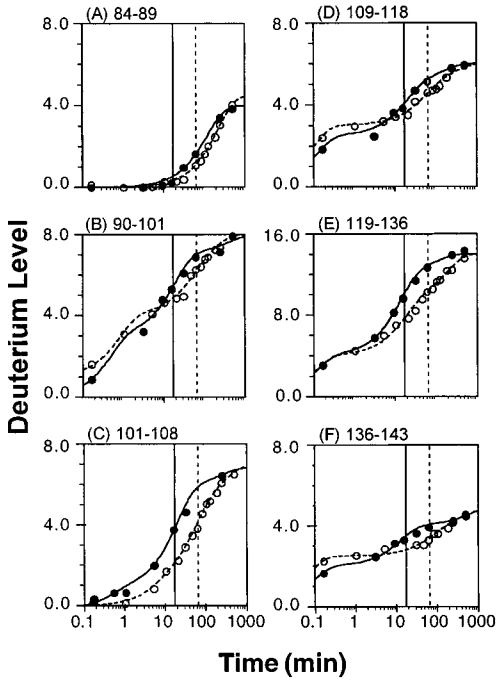


FIGURE 6: Deuterium exchange in curves for six peptides produced by peptic digestion of Hck SH3 alone (●) and Hck SH3 with HIV Nef peptide (○). The NefP concentration was 9500 $\mu$M. Vertical solid and dashed lines indicate the $t_{1/2}$ found for SH3 alone and SH3 with NefP, respectively, with intact protein analysis.

residues, it follows that peptide amide hydrogens in other segments must also participate in the cooperative unfolding event. These amide hydrogens may be close in tertiary structure but distant in primary structure.

*Binding of HIV Nef Peptide Alters SH3 Unfolding Dynamics.* Association of Hck SH3 with the HIV Nef protein is the tightest known SH3 interaction ($K_D$ 0.25 $\mu$M) and involves the Nef PxxP motif as well as other tertiary interactions (*11*, *50*). A peptide comprising residues 69−80 of HIV Nef, which includes the PxxP motif, binds Hck SH3 with a $K_D$ of 90 $\mu$M (*11*). To understand how binding of HIV Nef to Hck SH3 might alter cooperative unfolding of SH3, hydrogen-exchange experiments were performed with Hck SH3 bound to NefP. Bimodal isotope patterns found in mass spectra of intact SH3 incubated with NefP (Figure 1B) suggest that a cooperative unfolding occurs similar to that found for SH3 in the absence of NefP, but at a much slower rate. To determine whether the apparent decrease in the rate of cooperative unfolding was attributable to the dynamics of the Hck SH3−HIV Nef peptide complex, or simply due to the decreased level of unbound SH3 in solution, the SH3 domain was incubated with various concentrations of NefP and analyzed as described above. A plot of $1/k_{app}$ (where $k_{app}$ is the observed or apparent rate constant) vs free peptide concentration will produce a straight line if there is no unfolding from the bound state (*48*). The plot of experimental results (Figure 7) is nonlinear, suggesting unfolding from both the unbound and bound forms of SH3. Fitting the experimental data with eq 3 describing unfolding from bound and unbound forms yields a $K_D$ value of 25 $\mu$M and a rate constant for unfolding from the bound form ($k_{-1}'$) of 0.011 min$^{-1}$ ($t_{1/2}$ 63 min). The data do not fit eq 3 if unfolding from the bound form is neglected (straight dotted line in Figure 7). The difference between the $K_D$ found in this study and that reported by Lee et al. (*11*) may

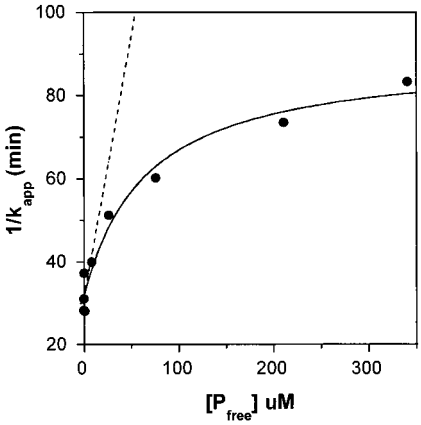


FIGURE 7: Evidence for unfolding of Hck SH3 from the bound state: plot of $1/k_{app}$, where $k_{app}$ is the observed rate constant, vs free peptide concentration. The experimental data were fitted with eq 3. The nonlinear plot indicates that unfolding from the bound state ($k_1'$ in eq 3) is significant. For no unfolding from the complex, the variation of $1/k_{app}$ with [P] would follow the dotted line.

be due to slightly different experimental conditions used in the two studies. In the presence of the Nef peptide, the difference between the centroids of the two peaks representing the folded and unfolded forms is 15 Da (Figure 2), 2 Da fewer than for the Hck SH3 domain alone. This observation suggests that the size of the unfolding unit in the complex is likely only slightly smaller than the size of the unfolding unit in unbound SH3.

Deuterium levels in peptic fragments derived from the SH3−NefP complex were determined as described above for the unbound domain (Figure 6). Dashed vertical lines in Figure 6 indicate a half-life for the cooperative unfolding of complexed SH3 of 63 min. As for unbound SH3, deuterium levels in the segment including residues 84−89 (Figure 6A) increase too slowly to be involved with the cooperative unfolding process. Deuterium levels in the other segments increase for incubation times of 63 min, indicating that residues located in several regions may be involved with the cooperative unfolding. However, deuterium levels in segments including residues 101−108 and 119−136 (Figure 6C,E) have the largest increases for incubation times around 63 min, suggesting that cooperative unfolding involves primarily residues from these regions. Moreover, the isotope patterns found for these segments appear binomial in the SH3−NefP complex (Figure 5B) just as they did for unbound SH3, providing further support for their involvement in cooperative unfolding of the SH3−NefP complex.

Important structural information about NefP binding can also be deduced from hydrogen exchange occurring through EX2 kinetics, which indicates localized stability (*51*). Binding of HIV Nef peptide alters hydrogen-exchange rates in regions of SH3 that are not involved in cooperative unfolding. For example, hydrogen exchange in residues 84−89 (Figure 6A) is significantly slower in the complex, suggesting that this region is more stable in the complex. In addition, at the shortest incubation time used in this study (0.16 min), intact unbound SH3 incorporated six fewer deuteriums than the bound form (Figure 2), indicating that binding destabilized at least six residues. Deuterium levels at the shortest incubation time in the three fragments including residues 90−101, 109−118, and 136−143 (Figure 6B,D,F) are higher in bound SH3, suggesting that binding destabilized several regions throughout SH3. Two of these regions, 90−101 and 109−118, are located directly in the binding site (see Figure 4). Thus, binding of NefP to Hck SH3 destabilizes some regions but stabilizes other regions.

## DISCUSSION

Unfolding of the N-terminal domain of Drk has been detected by NMR (*18*, *19*). Drk, an adapter protein from *Drosophila*, has an exchange rate of about 1 $s^{-1}$ at pH 7. It has been postulated that low stability of the SH3 domain may result from its loss of contact with other parts of the same protein or with other proteins (*21*). *In vivo* the N-terminal SH3 domain from Drk is part of the larger Drk protein and is constitutively associated with its target protein Sos (*52*) where it may be stabilized by interdomain or interprotein associations. The importance of this form of stabilization is supported by NMR studies detecting no equilibrium between folded and unfolded states for the Drk homologue in mammals, the N-terminal SH3 domain of Grb2, when bound to a proline-rich peptide (*53*, *54*). However, stabilization does not necessarily mean that the domain is no longer fluctuating. We have shown with hydrogen exchange and mass spectrometry that the Hck SH3 domain, which appears to be stable in 2D NMR experiments (*55*), does in fact unfold, but on a time scale that would make it appear stable in NMR experiments. We also show that even in one of the tightest SH3−peptide associations, Hck SH3 interacting with HIV Nef peptide (*11*), unfolding still occurs. It is quite possible that Drk and Grb2, as well as other SH3 domains and perhaps a myriad of other proteins, unfold in a similar slow manner, even when complexed with peptides or target proteins.

Bimodal isotope patterns characteristic of EX1 hydrogen-exchange kinetics are the basis of a new experimental method useful for detecting slow unfolding processes. This approach is attractive because although EX1 kinetics can be distinguished by NOE-based NMR, hydrogen exchange and mass spectrometry provide the most direct evidence for EX1 kinetics (*40*). Detecting HX by mass spectrometry is also attractive because (1) localized unfolding can be detected on time scales ranging from seconds to days, (2) localized unfolding in very large proteins can be studied (*41*, *56*, *57*), and (3) the measurements can be performed with substantially less material than is required for NMR. We have demonstrated effectiveness of this method by determining the rate of slow localized unfolding for Hck SH3, first with intact protein analysis and then with analysis of small peptic fragments. Correlation between the rates of unfolding, determined by analyzing both the intact SH3 domain and its peptic fragments, indicates which fragments may be involved with unfolding.

The most distinguishing characteristic of fragments involved with unfolding is the appearance of EX1 patterns in their mass spectra. Two fragments displayed this EX1 or bimodal isotope pattern: 101−108 and 119−136. In these bimodal isotope patterns, the folded or less deuterated state is indicated by the lower envelope, while the unfolded or more deuterated state is indicated by the higher envelope. The mass difference between the centroids of the two envelopes indicates how many amide hydrogens are involved in unfolding of a particular segment. When the number of amide hydrogens that are involved is small, the two envelopes may merge together, preventing accurate analysis.

This is the case for fragment 101−108 where the isotope envelopes are evident, but accurate determination of the centroid of each envelope is not possible. The difference between the isotopic envelopes for fragment 119−136 can be determined more accurately because a larger part of this segment participates in the cooperative unfolding event. Recognizing these limitations in our analysis of the bimodal isotope patterns found for segments 101−108 and 119−136, we suggest that these segments include 9−11 residues that participate in the cooperative unfolding event. Analysis of the intact protein indicates that at least 17 amide hydrogens are involved with unfolding. The difference between these estimates suggests that the cooperative unfolding event involves several short segments of the SH3 backbone. Although these short segments are not contiguous along the backbone, they must have strong interactions in the folded protein. Unfortunately, the spatial resolution afforded by the peptic fragments is not sufficient to locate the interacting segments more accurately.

Based on our results, regions of Hck SH3 primarily involved in cooperative unfolding include residues 101−108 and 119−136. Most of these residues are not directly in the SH3 binding site but are positioned to influence its conformation. Residues 101−108 make up the last part of the RT-loop and are on the opposite side of the loop from the binding site (see Figure 4). Some residues in the 119−136 segment form a portion of the binding region, while a majority of residues in this segment are distant from the binding site. Segment 119−136, which forms an antiparallel $\beta$-sheet from $\beta$-strands $\beta$c and $\beta$d, also has several amide hydrogens bonded to residues in the RT-loop. Unfolding of this $\beta$-sheet would likely alter the binding site conformation.

How might slow, cooperative unfolding of SH3 be used to control kinase activity? Mutational analysis (*58*) has shown that key residues in the n-Src- and RT-loops of SH3 domains are required for intermolecular interactions of SH3 with target proteins *in vivo*. The crystal structure of Hck (*9*) has shown intramolecular interactions of n-Src- and RT-loops with the SH2−kinase linker and kinase domain that are likely required to suppress kinase activity. Our results show for the first time that a substantial part of SH3 undergoes slow, cooperative unfolding. The critical question of whether this unfolding might release SH3 ligands remains unanswered. If unfolding does not release the ligand, it may have no biological significance. However, if unfolding does release the ligand, it may have substantial biological significance. Ligand release upon unfolding provides a mechanism for kinetics to intervene in the normal thermodynamic control of Hck activity by decreasing the time required to respond to an external stimulus. For example, if the SH2−kinase linker binds tightly, a long time may be required to re-establish equilibrium concentrations of active and inactive Hck when the concentration of an external ligand changes. SH3 unfolding may permit release of the SH2−kinase linker ligand in the closed, inactive form of Hck kinase, allowing access to other SH3 ligands. Once the SH3 domain is released and bound to another substrate, the return of the kinase to the inactive form is dependent on the unfolding/ligand-release capacity of SH3 in its new complex. As we have shown, Nef peptide slows the SH3 unfolding process. Because full length Nef has more interaction with SH3 than Nef peptide alone (*50*), it probably slows SH3 unfolding even more. As a result, intermolecular interactions between the SH3 domain and HIV Nef (or other target molecules) may stabilize SH3 and prevent unfolding and ligand release thereby decreasing the rate of SH3 reassociation with the SH2−kinase linker and maintaining an active kinase conformation.

Biological data support this view. Binding of Nef to Hck SH3 is sufficient to constitutively activate Hck *in vivo* and leads to a transformed phenotype in fibroblasts (*13*). Without the inherent SH3 flexibility and release of the SH2−kinase linker, the intramolecular interaction with the SH2−kinase linker region may persist and prevent SH3-dependent kinase activation. The significance to Hck regulation of unfolding/ligand release and intervening in thermodynamic control can only be determined when $k_{on}$ and $k_{off}$, as well as the effective concentrations of SH2−linker and Nef, are known. One of the first steps in determining the biological significance of the slow unfolding of SH3 will be to determine whether this process occurs for SH3 in its native environment as a constituent of intact Hck. These experiments are not outside the bounds of the experimental methods used in this study, which have been used to study much larger proteins (*41*, *56*, *57*).

## ACKNOWLEDGMENT

We would like to thank Nancy Dunham for help with domain purification.

## REFERENCES

1. Nimmesgern, E., Fox, T., Fleming, M. A., and Thomson, J. A. (1996) *J. Biol. Chem. 271*, 19421−19427.
2. Creighton, T. E. (1992) in *Protein Folding* (Creighton, T. E., Ed.) W. H. Freeman and Co., New York.
3. Wilson, I. A., and Stanfield, R. L. (1994) *Curr. Opin. Struct. Biol. 4*, 857−867.
4. Spolar, R. S., and Record, M. T., Jr. (1994) *Science 263*, 777−784.
5. Kriwacki, R. W., Hengst, L., Tennent, L., Reed, S. I., and Wright, P. E. (1996) *Proc. Natl. Acad. Sci. U.S.A. 93*, 11504−11509.
6. Shen, F., Triezenberg, S. J., Hensley, P., Porter, D., and Knutson, J. (1996) *J. Biol. Chem. 271*, 4827−4837.
7. Alexandrescu, A. T., Abeygunawardana, C., and Shortle, D. (1994) *Biochemistry 33*, 1063−1072.
8. Pawson, T. (1995) *Nature 373*, 573−580.
9. Sicheri, F., Moarefi, I., and Kuriyan, J. (1997) *Nature 385*, 602−609.
10. Xu, W., Harrison, S. C., and Eck, M. J. (1997) *Nature 385*, 595−602.
11. Lee, C.-H., Leung, B., Lemmon, M. A., Zheng, J., Cowburn, D., Kuriyan, J., and Saksela, K. (1995) *EMBO J. 14*, 5006−5015.
12. Moarefi, I., LaFevre-Bernt, M., Sicheri, F., Huse, M., Lee, C.-H., Kuriyan, J., and Miller, W. T. (1997) *Nature 385*, 650−653.
13. Briggs, S. D., Sharkey, M., Stevenson, M., and Smithgall, T. E. (1997) *J. Biol. Chem. 272*, 17899−17902.
14. Chen, Y.-J., Lin, S.-C., Tzeng, S.-R., Patel, H. V., Lyu, P.-C., and Cheng, J.-W. (1996) *Proteins: Struct. Funct. Genet. 26*, 465−471.
15. Viguera, A. R., Martinez, J. C., Filimonov, V. V., Mateo, P. L., and Serrano, L. (1994) *Biochemistry 33*, 2142−2150.
16. Lim, W. A., Fox, R. O., and Richards, F. M. (1994) *Protein Sci. 3*, 1261−1266.
17. Privalov, P. L. (1979) *Adv. Protein Chem. 33*, 167−241.
18. Zhang, O., and Forman-Kay, J. D. (1995) *Biochemistry 34*, 6784−6794.
19. Farrow, N. A., Zhang, O., Forman-Kay, J. D., and Kay, L. E. (1995) *Biochemistry 34*, 868−878.

20. Goudreau, N., Cornille, F., Duchesne, M., Parker, F., Tocque, B., Garbay, C., and Roques, B. P. (1994) *Nature Struct. Biol. 1*, 898−907.
21. Farrow, N. A., Zhang, O., Forman-Kay, J. D., and Kay, L. E. (1997) *Biochemistry 36*, 2390−2402.
22. Zhang, O., and Forman-Kay, J. D. (1997) *Biochemistry 36*, 3959−3970.
23. Morton, C. J., Pugh, D. J. R., Brown, E. L. J., Kahmann, J. D., Renzoni, D. A. C., and Campbell, I. D. (1996) *Structure 4*, 705−714.
24. Hiroaki, H., Klaus, W., and Senn, H. (1996) *J. Biomol. NMR 8*, 105−122.
25. Gosser, Y. Q., Zheng, J., Overduin, M., Mayer, B. J., and Cowburn, D. (1995) *Structure 3*, 1075−1086.
26. Yu, H., Rosen, M. K., and Schreiber, S. L. (1993) *FEBS Lett. 324*, 87−92.
27. van Aalten, D. M. F., Amadei, A., Bywater, R., Findlay, J. B. C., Berendsen, H. J. C., Sander, C., and Stouten, P. F. W. (1996) *Biophys. J. 70*, 684−692.
28. Borchert, T. V., Mathieu, M., Zeelen, J. P., Courtneidge, S. A., and Wierenga, R. K. (1994) *FEBS Lett. 341*, 79−85.
29. Musacchio, A., Saraste, M., and Wilmanns, M. (1994) *Nature Struct. Biol. 1*, 546−551.
30. Booker, G. W., Gout, I., Downing, A. K., Driscoll, P. C., Boyd, J., Waterfield, M. D., and Campbell, I. D. (1993) *Cell 73*, 813−822.
31. Loh, S. N., Rohl, C. A., Kiefhaber, T., and Baldwin, R. L. (1996) *Proc. Natl. Acad. Sci. U.S.A. 93*, 1982−1987.
32. Bai, Y., Sosnick, T. R., Mayne, L., and Englander, S. W. (1995) *Science 269*, 192−197.
33. Mayo, S. L., and Baldwin, R. L. (1993) *Science 262*, 873−876.
34. Kim, K.-S., and Woodward, C. (1993) *Biochemistry 32*, 9609−9613.
35. Thévenon-Emeric, G., Kozlowski, J., Zhang, Z., and Smith, D. L. (1992) *Anal. Chem. 64*, 2456−2458.
36. Katta, V., and Chait, B. T. (1991) *Rapid Commun. Mass Spectrom. 5*, 214−217.
37. Johnson, R. S., and Walsh, K. A. (1994) *Protein Sci. 3*, 2411−2418.
38. Zhang, Z., and Smith, D. L. (1993) *Protein Sci. 2*, 522−531.
39. Smith, D. L., Deng, Y., and Zhang, Z. (1997) *J. Mass Spectrom. 32*, 135−146.
40. Miranker, A., Robinson, C. V., Radford, S. E., Aplin, R. T., and Dobson, C. M. (1993) *Science 262*, 896−900.
41. Zhang, Z., Post, C. B., and Smith, D. L. (1996) *Biochemistry 35*, 779−791.
42. Dharmasiri, K., and Smith, D. L. (1996) *Anal. Chem. 68*, 2340−2344.
43. Bai, Y., Milne, J. S., Mayne, L., and Englander, S. W. (1993) *Proteins: Struct. Funct. Genet. 17*, 75−86.
44. Zhou, Z., and Smith, D. L. (1990) *J. Protein Chem. 9*, 523−532.
45. Biemann, K. (1990) *Methods Enzymol. 193*, 455−479.
46. Caprioli, R. M., and Fan, T. (1986) *Anal. Biochem. 154*, 596−603.
47. Smith, J. B., Sun, Y., Smith, D. L., and Green, B. (1992) *Protein Sci. 1*, 601−608.
48. Sancho, J., Meiering, E. M., and Fersht, A. R. (1991) *J. Mol. Biol. 221*, 1007−1014.
49. Woodward, C., Simon, I., and Tuchsen, E. (1982) *Mol. Cell. Biochem. 48*, 135−160.
50. Lee, C.-H., Saksela, K., Mirza, U. A., Chait, B. T., and Kuriyan, J. (1996) *Cell 85*, 931−942.
51. Bai, Y. W., Milne, J. S., Mayne, L., and Englander, S. W. (1994) *Proteins: Struct. Funct. Genet. 20*, 4−14.
52. Schlessinger, J. (1993) *Trends. Biochem. Sci. 18*, 273−275.
53. Wittekind, M., Mapelli, C., Farmer, B. T., II, Suen, K.-L., Goldfarb, V., Tsao, J., Lavoie, T., Barbacid, M., Meyers, C. A., and Mueller, L. (1994) *Biochemistry 33*, 13531−13539.
54. Terasawa, H., Kohda, D., Hatanaka, H., Tsuchiya, S., Ogura, K., Nagata, K., Ishii, S., Mandiyan, V., Ullrich, A., Schlessinger, J., and Inagaki, F. (1994) *Nature Struct. Biol. 1*, 891−898.
55. Gmeiner, W. H. (unpublished results).
56. Zhang, Z., and Smith, D. L. (1996) *Protein Sci. 5*, 1282−1289.
57. Liu, Y., and Smith, D. L. (1994) *J. Am. Soc. Mass Spectrom. 5*, 19−28.
58. Erpel, T., Superti-Furga, G., and Courtneidge, S. A. (1995) *EMBO J. 14*, 963−975.

BI971635M